Corresponding Author: Professor Valentina Anna Lia Salomoni, PhD, Post-
Doc

Corresponding Author's Institution: University of Padua

First Author: Gianluca Mazzucco

Order of Authors: Gianluca Mazzucco; Beatrice Pomaro; Valentina Anna Lia
Salomoni, PhD, Post-Doc; Carmelo E Majorana

Abstract: Within the framework of numerical algorithms for the three-
dimensional random packing of granular materials this work presents an
innovative formulation for polydispersed ellipsoidal particles, including
an overlapping detection algorithm for an optimized simulation of the
mesostructure of geomaterials, particularly concrete.
Granular composite cement-based materials can be so reconstructed with
adequate precision in terms of grain size distribution. Specifically, the
algorithm performance towards the assumed inclusion shape (ellipsoidal or
spheric) and degree of regularity (round or irregular) is here discussed.
Examples on real grading curves prove that this approach is effective.
The advantages of the proposed method for computational mechanics
purposes are also disclosed when properly interfaced with visualization
CAD (Computer Aided Design) tools.

Cover Letter

DIPARTIMENTO DI INGEGNERIA CIVILE, EDILE E AMBIENTALE - I C E A
DEPARTMENT OF CIVIL, ENVIRONMENTAL AND ARCHITECTURAL ENGINEERING

Via F. Marzolo, 9 - I 35131 Padova
tel +39 049 8275424 fax +39 049 8275446

C.F 80006480281 - P.IVA 007 42430283

Padua, December 5th 2017

To the Editor of
Construction and Building Materials

Dear Editor,

Please find enclosed the revised version of the original manuscript:

Numerical modelling of ellipsoidal inclusions
By G. Mazzucco, B. Pomaro, V.A. Salomoni, C.E. Majorana

for possible publication in Your Journal.

Yours Sincerely,

Valentina Salomoni
on behalf of all authors

CONBUILDMAT-S-17-07052

Response to Reviewer #2

The paper deals with the proposal of a numerical algorithm for spatially generating ellipsoidal inclusions within a three-dimensional domain. Different packing densities are obtained following real grading curves.

Some aspects need to be better explained:

- *Can this method be applied to other different aggregate types besides natural aggregates, e.g. graded aggregates?*

At this stage, the algorithm is able to handle ellipsoidal geometries only and for this reason the method is more reliable when the inclusions are given by natural aggregates. Anyway it can be applied even if graded aggregates are considered, having in mind that a slightly higher error in calculating volumes could occur.

- *Please clarify why three different shape ratios have been considered in the example of Section 5.1*

Based on the grading curves developed in Ref. [30], the aggregate shape ratios are not given. For this reason, when numerically reproducing this experimental case, we have assumed three different shape ratios for each sieve: two characterized by the maximum and minimum dimension, respectively, which are necessary to retain the corresponding passing of a given aggregate, and a third shape ratio which is an average between the first two configurations. Three shape ratios have been considered for each sieve in order to realistically diversify the aggregate shape ratios of the grading curve in a reasonable way.

- *Why have coarse aggregates been taken into account only? Is it possible to consider also the fine part of a grading curve in the analyses?*

In principle the described procedure is able to reproduce the whole grading curve, i.e. coarse and fine aggregates. However, considering that the fine part would lead to a very large number of inclusions and a huge computational effort without a considerable benefit in the numerical simulation of the real grading curve, the coarse part only has been taken into account.

Moreover, as explained at the end of Section 1, the algorithm is aimed to reproduce samples at a meso-scale level; at this scale the coarse fraction is the one referred as aggregates, being particles of diameter less than 5mm generally included within the cement paste.

CONBUILDMAT-S-17-07052

Response to Reviewer #3

The paper is interesting and only few modifications are required.

There should be a space between a number and the appropriate unit, for example 1 mm, not 1mm. Moreover, the units should not be in italic font.

The manuscript has been corrected

page 3, line 45: ... and the the divide ...
page 5, line 85: approximated to -> approximated by
page 7, above equation (11): ... there exists a position vector exists satisfying ...
page 8, lines 103 and 104: it is not clear that \lambda is from the space R^3. \lambda is a value, it is not a vector.
page 9, line 119: mesostracture -> mesostructure
page 11, line 168: algorith -> algorithm
page 18, line 247: originary > originally

Please consider the corrections within the paper

*Highlights

> Algorithm for randomly distributing 3D inclusions. > Employment of real grading curves.　> Effective simulation of different packing densities. > Novel dislocation procedure. > Procedure suitable for modelling composite materials.

Numerical modelling of ellipsoidal inclusions

G. Mazzucco[a], B. Pomaro[a], V.A. Salomoni[a,b,*], C.E. Majorana[a]

[a]*Department of Civil, Environmental and Architectural Engineering (DICEA),
University of Padova, Via F. Marzolo 9, 35131 Padova, Italy.*
[b]*Department of Management and Engineering (DTG),
University of Padova, Stradella S. Nicola 3, 36100 Vicenza, Italy.
E-mail addresses: gianluca.mazzucco@dicea.unipd.it; beatrice.pomaro@dicea.unipd.it;
valentina.salomoni@dicea.unipd.it; carmelo.maiorana@dicea.unipd.it.*

Abstract

Within the framework of numerical algorithms for the three-dimensional random packing of granular materials this work presents an innovative formulation for polydispersed ellipsoidal particles, including an overlapping detection algorithm for an optimized simulation of the mesostructure of geomaterials, particularly concrete.

Granular composite cement-based materials can be so reconstructed with adequate precision in terms of grain size distribution. Specifically, the algorithm performance towards the assumed inclusion shape (ellipsoidal or spheric) and degree of regularity (round or irregular) is here discussed. Examples on real grading curves prove that this approach is effective.

The advantages of the proposed method for computational mechanics purposes are also disclosed when properly interfaced with visualization CAD (Computer Aided Design) tools.

Keywords: Random ellipsoidal inclusions, mesostructure, random packing algorithm, grain size distribution.

**Corresponding author
Email address:* `valentina.salomoni@dicea.unipd.it` (V.A. Salomoni)

1. Introduction

The packing density can strongly influence the performance of granular materials like concrete and the costs related to its production. The basic concept of a packing method is to minimize the voids content by studying an optimum mixture of coarse and fine aggregates, so minimizing the amount of the required binder and water in the mix. The packing of a cementitious material depends basically on the aggregates size and shape and on the applied packing method itself. While the first parameter is determined by choosing recommended grading curves and the latter is easily guaranteed by a satisfactory vibration during casting, the second one can not always be optimized since it is strictly related to aggregate availability. He et al. [1] demonstrated for mono-sized particles that polyhedra with larger sphericity can be packed to a higher density. Sphericity is defined as the surface area ratio of a sphere with a particle, equivalent in volume. Xu and Chen [2] reached a similar conclusion for polydispersed ellipsoidal particles. Similarly in 2D, Xu et al. [3] found that, when ellipses slightly deviate from circles, the packing fraction rises to the maximum value, otherwise it decreases.

When numerically modeling concrete at the mesoscopic scale, i.e. at the scale of its constituents, it is significant to reproduce the real particle packing which is related to the w/c ratio and therefore, practically, to concrete workability and final strength.

The packing of spheres was first theoretically and experimentally investigated in [4] for mixes with very large size difference between the fine and coarse particles. Later Stovall et al. [5] developed a model to predict the packing density of multi-sized grain mixtures, including the loosening and wall effects, i.e. taking into account particle interactions and interactions of the particles at the boundaries.

With the advances in computer simulations many works have focused on the development of algorithms for the random distribution of non-overlapping particles. In most studies the assumption of spherical aggregates is made for sake

2

of simplicity [6-8], however some works deal with more complex geometries, e.g. Wittmann et al. [9] generated 2D rounded aggregates by using the morphological law developed by Beddow and Meloy [10] and angular aggregates as polygons, of randomly varying number of edges and angles; more recently Wang et al. [11] developed a procedure for generating random aggregate structures for rounded and angular aggregates based on Wittmann's findings but here angular aggregates are generated as polygons with prescribed elongation ratios, rather than just as randomly shaped polygons. Three-dimensional studies involving ellipsoids are reported in [12-15], while Williams and Philipse [16] used spherocylinders to better simulate the elongation of real particles, such as fibers.

As regards the packing algorithm, two are mainly adopted in the scientific literature: the take-and-place method [9, 11, 17], which consists in randomly positioning a number of particles necessary to satisfy the sieving classes in which the grading curve can be divided, proceeding from large to small particles; and the divide-and-fill method [18], which consists in subdividing the whole domain in 2D or 3D into sub-regions and fill them with grain particles, based on the grading curve and the aggregate fraction. An optimized algorithm to pack very large volumes of spherical entities, enriched by a genetic module, has been more recently developed in [7]: this method is derived from [19] and it is found to significantly improve the speed of convergence of the sequential packing algorithm of spheres. In line with a "parent-child" model, it adaptively shifts and shrinks the search space in the control volume by employing feasible (with satisfied constraints) and infeasible (with unsatisfied constraints) spheres in the population of "children" to find a sphere with maximum radius. By doing so the module can search the free space within a domain to inscribe the maximum-sized spheres among the previously packed ones, in an optimal way.

Within this framework the work proposes an original, mathematically-based formulation for the ellipsoidal particle size distribution within a 3D space and it discusses its performance when spherical inclusions are employed. The method takes inspiration from the divide-and-fill method but it is improved by the introduction of a control step of new concept and implementation, which allows

3

further packing and an optimized use of the free available space. The study is directed towards a three-dimensional modeling of cement-based composite materials at the mesocopic scale in order to manage space discretization in agreement with the Finite Element Method (FEM) and perform numerical analyses in the context of continuum mechanics [20].

2. Grading curves in concrete materials

The size distribution of aggregate particles in concrete can be defined either by means of grading curves or from sieve analyses.

Several types of ideal grading curves can be applied, the most known and acceptable of them is Fuller's curve [21], which is described by a simple equation relating the percentage of aggregates passing through one sieve P_i to the corresponding sieve diameter d_i and the maximum dimension of the aggregates D_{max}:

$$P_i = 100\sqrt{d_i/D_{max}}.$$ (1)

It is well known that Fuller's curve gives good results for low-workability mixes. To obtain a better compaction maintaining a good workability, Bolomey's curve [22] is to be preferred. Equation (1) is modified according to Bolomey into:

$$P_i = A + (100 - A)\sqrt{d_i/D_{max}}$$ (2)

where the parameter A accounts for the impact of adding fine particles in the mix and it derives from imposing an arbitrary percentage A at the 80 μm sieve. In general, grading curves do not consider the geometry of aggregates, but only the maximum diameter and that related to the current passing percentage. However the geometry must play a role in the compaction process which can not be neglected when modeling a mesoscopic structure that resembles the real one.

European standards [23] give some indications on how to determine the shape index of coarse aggregates; the method applies for natural or artificial aggregates, including lightweight aggregates, and it classifies an aggregate according

4

to two main dimensions: the length of a grain L and its thickness E, defined respectively as the maximum and the minimum distance between two parallel planes tangential to the particle surface. An aspect ratio L/E greater than 3 accounts for *non-cubic* particles and, in this sense, the test leads to the evaluation of the percentage of *cubic* or *non-cubic* grain fractions of a given mix.
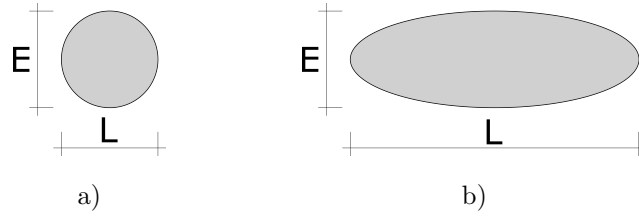

Figure 1: Aggregate ratio $L/E = 1$; aggregate ratio $L/E = 3$.

If one accepts that, in line with the European standard, the *non-cubic* condition defines the usability limit of aggregates in a mix, particles with ratio $1 \leq L/E \leq 3$ can be conveniently approximated by ellipsoids more than spheres (for which $L/E = 1$) and in this range an ellipsoidal representation is still acceptable; it may be not so for higher L/E ratios.
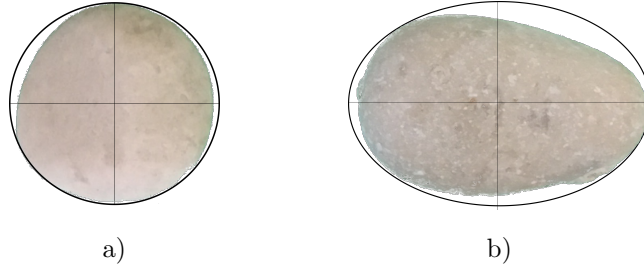

Figure 2: Spheric aggregate a); ellipsoidal aggregate b).

3. Theoretical background

3.1. Ellipsoidal formulation

An ellipsoid surface satisfies the following equation:

$$f(\mathbf{x}) = \frac{x^2}{l_x^2} + \frac{y^2}{l_y^2} + \frac{z^2}{l_z^2} - 1 = 0 \tag{3}$$

5

where x, y, z are the position vector components of vector: $\mathbf{x} = [x, y, z]^T$ while $\mathbf{l} = [l_x, l_y, l_z]$ are the semidiameters of the ellipses obtained by sectioning the ellipsoids with the coordinate planes.
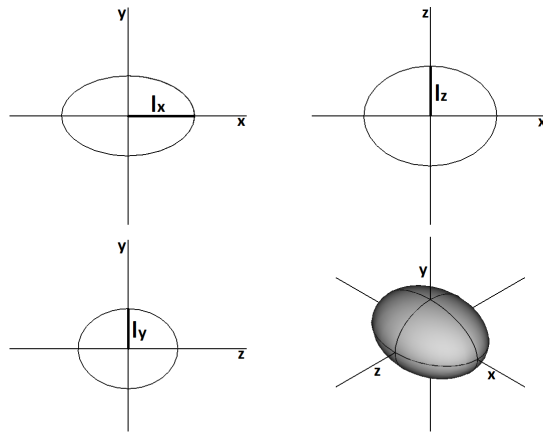

Figure 3: Sectioned ellipsoid.

Equation (3) in matrix notation yields [24]:

$$f(\mathbf{x}) = \mathbf{x}^T \mathbf{B} \mathbf{x} \tag{4}$$

where $\mathbf{B}$ is the associated matrix:

$$\mathbf{B}(\mathbf{l}) = \begin{bmatrix} 1/l_x^2 & 0 & 0 & 0 \\ 0 & 1/l_y^2 & 0 & 0 \\ 0 & 0 & 1/l_z^2 & 0 \\ 0 & 0 & 0 & -1 \end{bmatrix} \tag{5}$$

rescaling the position vector $\mathbf{x}$ as $\mathbf{x}^T = [x, y, z, 1]^T$.

In this "standard" notation, the ellipsoid is centered in the Cartesian reference system and the principal axes are the coordinate axes.

Any rotated or translated ellipsoid is obtained by applying the rotational $\mathbf{R}$ and

6

translational $\mathbf{T}$ operators to this initial configuration:

$$\mathbf{R(e)} = \begin{bmatrix} e_{1x} & e_{2x} & e_{3x} & 0 \\ e_{1y} & e_{2y} & e_{3y} & 0 \\ e_{1z} & e_{2z} & e_{3z} & 0 \\ 0 & 0 & 0 & 1 \end{bmatrix} \quad \mathbf{T(o)} = \begin{bmatrix} 1 & 0 & 0 & 0 \\ 0 & 1 & 0 & 0 \\ 0 & 0 & 1 & 0 \\ -o_x & -o_x & -o_z & 1 \end{bmatrix} \tag{6}$$

where $\mathbf{e} = [\mathbf{e}_1, \mathbf{e}_2, \mathbf{e}_3]$ is the base vector for the new reference system and $\mathbf{o}$ is the new centre.

Therefore the most general expression for the equation of an ellipsoid arbitrarilly oriented in a 3D space is:

$$\mathbf{x}^T \mathbf{M} \mathbf{x} = 0 \tag{7}$$

where $\mathbf{M}$ is the generic ellipsoid matrix after roto-translation, which can be defined as $\mathbf{M} = \mathbf{R}(\mathbf{TBT}^T)\mathbf{R}^T$ in agreement with [25].

3.2. A criterion for detecting overlapping of ellipsoidal particles

At this step, given two ellipsoids E_0 and E_1 defined by their associated matrices $\mathbf{M}_0$ and $\mathbf{M}_1$, respectively, the functions of the external surfaces are defined by:

$$\mathbf{x}^T \mathbf{M}_0 \mathbf{x} = 0 \quad ; \quad \mathbf{x}^T \mathbf{M}_1 \mathbf{x} = 0 \tag{8}$$

while the solid volumes satisfy the following inequalities:

$$\mathbf{x}^T \mathbf{M}_0 \mathbf{x} < 0 \quad ; \quad \mathbf{x}^T \mathbf{M}_1 \mathbf{x} < 0. \tag{9}$$

The E_0 function can be rewritten with a multiplying scalar factor λ without loss in generality:

$$\mathbf{x}^T \lambda \mathbf{M}_0 \mathbf{x} = 0. \tag{10}$$

If the two ellipsoids E_0 and E_1 overlap on a region in space it means that there exists a position vector $\mathbf{x}^*$ satisfying both Equations (9) which yields to:

$$\mathbf{x}^{*T}(\lambda \mathbf{M}_0 - \mathbf{M}_1)\mathbf{x}^* = \mathbf{x}^{*T} \mathbf{M}_0 (\lambda \mathbf{I} - \mathbf{M}_0^{-1}\mathbf{M}_1)\mathbf{x}^* = 0. \tag{11}$$

This relationship admits a solution if:

$$det\left(\mathbf{M}_0(\lambda\mathbf{I} - \mathbf{M}_0^{-1}\mathbf{M}_1)\right) = 0 \tag{12}$$

but (12) represents an eigenvalues/eigenvectors problem where the parameters λ_i are the eigenvalues. Based on the values they assume, specific relationships between the ellipsoidal inclusions are envisaged [25, 26]: if all the $\lambda_i > 0 \in \mathbb{R}$, then one ellipsoid properly contains the other, i.e. they totally penetrate each other; if some $\lambda_i < 0 \in \mathbb{R}$, then the two ellipsoids are separated (a plane exists for which the ellipsoids are on opposite sides); finally, if all the λ_i are complex (all $\lambda_i \in \mathbb{C}$), then the two ellipsoids intersect, i.e. they overalp in some parts.
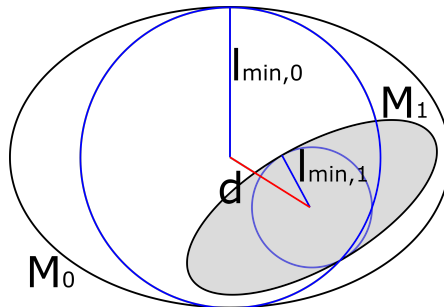

Figure 4: Penetration condition between two ellipsoids in 2D.

An algorithm aimed to randomly distribute in space non-intersecting ellipsoidal inclusions should prevent the occurrence of the first and the third case above. Particularly, to exclude the condition in which an ellipsoid contains the other, as reported in Fig. 4, a simple check can be implemented: given the position vectors of the centres of the two ellipsoids, $\mathbf{x}_0$ and $\mathbf{x}_1$, if the distance d between the two centres is less than the sum of the two minimum radii $l_{min,0}$, $l_{min,1}$, i.e.:

$$d = |\mathbf{x}_1 - \mathbf{x}_0| < l_{min,0} + l_{min,1} \tag{13}$$

then the two ellipsoids penetrate each other and one contains the other.

The second unforeseen event is avoided by applying the overlapping detection algorithm represented by Equation (12) and more directly by analysing the roots.

8

3.3. Random distribution of the mesostructure

The grading curve for a specific mix design determines the maximum number of ellipsoids that can be randomly placed in a sample, i.e. a control volume CV, in relation to the real volume fraction.

For example, by taking into account a CV of volume V_c and a maximum aggregate percentage equal to $p_\%$ of the CV, the required total volume of aggregates equals $V_a = p_\% V_c$. In agreement with the grading curve, being V_a known, the single volume fraction for each aggregate nominal dimension V_{ai} can finally be determined.

In the following an algorithm for the random generation of the mesostructure of concrete is conceptually outlined, while its numerical implementation is discussed in the next Section.

A first trial random configuration can be found by placing the inclusions one by one in the CV (starting from the largest), avoiding penetration and intersection with pre-existing particles. When ellipsoidal inclusions are considered, a random distribution is guaranteed provided that each ellipsoid is characterized by a randomly defined position of its centre in space and random rotations of the principal axes, which can be easily obtained via a random generator tool.

The location of a particle which is non-intersecting may require a maximum number of trials (N_{max}) and if the trials overcome N_{max} then the N_{max}-th aggregate is discarded. At this point two ways are possible: i) another ellipsoid is randomly generated and the positioning scheme is repeated until a first randomly defined ellipsoid with successful placement, or ii) the discarded ellipsoid is actually retained, provided that the intersecting particles in the neighbourhood are shifted of a certain amount in a way that no intersection occurs with the retained inclusion and the sorrounding particles.

The latter approach, called *dislocation* procedure, is here implemented; it is inspired by the "Metropolis scheme" reported in [27] and it is proved to be more efficient than the first one, for particle distribution purposes.

For sake of simplicity a 2D dislocation sequence is reported in Fig. 5: starting from an initial configuration (Fig. 5 a), the last possible N_{max}-th randomly

9

generated trial inclusion is found to intersect some surrounding particles (Fig. 5 b, c), therefore this inclusion is retained even if not successful, and the intersecting particles in the neighbourhood are moved opposite to the centre of the "unlucky" inclusion (the shift direction given by the unit vector **n**), until the non-intersecting check is satisfied, i.e. the imposed shifts of the surrounding particles equal the sum of the radius of the sphere circumscribed to the "unlucky" inclusion and the radius of the sphere circumscribed to the intersecting particle itself (i.e. tangency condition between circumscribed spheres, (Fig. 5 d). A translation is retained if, in the new configuration, the shifted inclusion does not overlap to any particle nearby; this must be satisfied by all the replaced surrounding particles (Fig. 5 e) before the trial inclusion is finally added (Fig. 5 f).
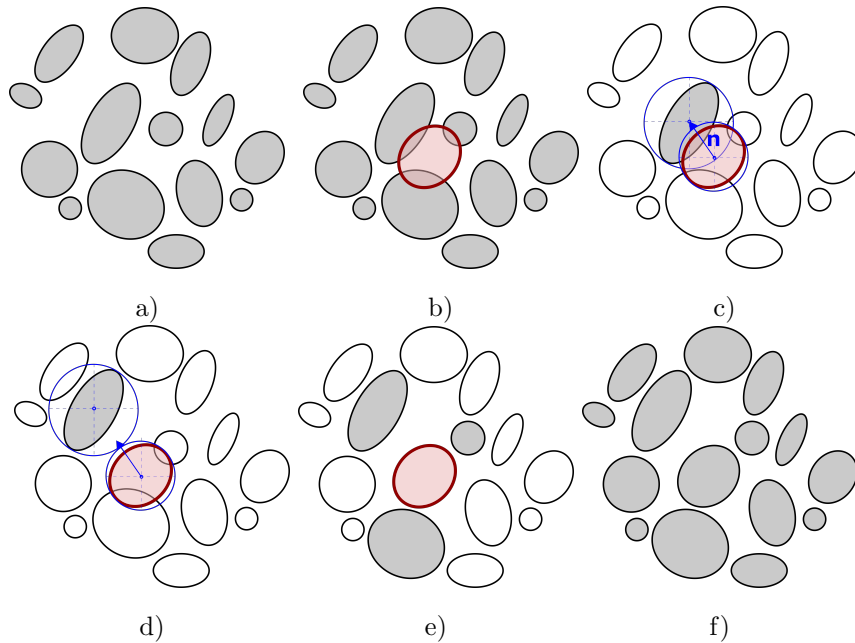

Figure 5: Dislocation sequence in a 2D configuration a)-f).

10

4. Numerical implementation

Once the dimensions of the parallelepiped sample, or CV, are defined, the proposed algorithm divides the domain in sub-domains in which the real grading curve has to be satisfied. The code can handle mesostructure simulations for cubic samples of 75 mm minimum edge, which is reasonable for cementitious materials, and a Bolomey's grading curve with a maximum sieve of 16 mm in diameter.

For each sub-domain the algorithm tries to place a specific ellipsoid, defined by Equations (3-7), with a random approach, i.e. with random position of centre and orientation of axes; the inclusions are defined in number for each sieve diameter by the grading curve. For each trial inclusion a check against intersection with prior particles is made through Equation (12) and against penetration through Equation (13), and the dislocation procedure is activated if some interferences between inclusions are detected when the trials to insert a new ellipsoid overcome N_{max}.

The illustrated algorithm has been implemented in *Visual Basic* language, which has allowed also the production of a user-friendly graphical interface for this tool (Fig. 6).

11

Random Aggregates Distribution

File   Edit   ?

Sample Dimensions

dimX = 75
dimY = 75
dimZ = 75

Grading Curve

%Agg Vol	lx(diameter)	ly	lz	Offsett	Part	Volume	n
5.0874	13	13	13	0.1	el_13_13_13	11804...	10
2.5437	13	12	9.1	0.1	el_13_12_9	5902.1...	7
2.5437	13	11	5.2	0.1	el_13_11_5	5902.1...	15
4.8786	10	10	10	0.1	el_10_10_10	11319...	21
2.4393	10	9	7	0.1	el_10_9_7	5659.9...	17
2.4393	10	8	4	0.1	el_10_8_4	5659.9...	33
3.9408	7	7	7	0.1	el_7_7_7	9143.8...	50
1.9704	7	6.5	4.9	0.1	el_7_6_4	4571.9...	39
1.9704	7	6	2.8	0.1	el_7_6_2	4571.9...	74
1.7462	5	5	5	0.1	el_5_5_5	4051.7...	61
0.8731	5	4.5	3.5	0.1	el_5_4_3	2025.8...	49
0.8731	5	4	2	0.1	el_5_4_2	2025.8...	96

Info

Vtot = 421875
Vagg = 232031.3
%tot = 49.866

Material

%Agg = 55

☐ Compaction

maxTry = 2
maxDis = 10
maxIter = 100

(plot: Agg Vol % vs Diameter — grading)
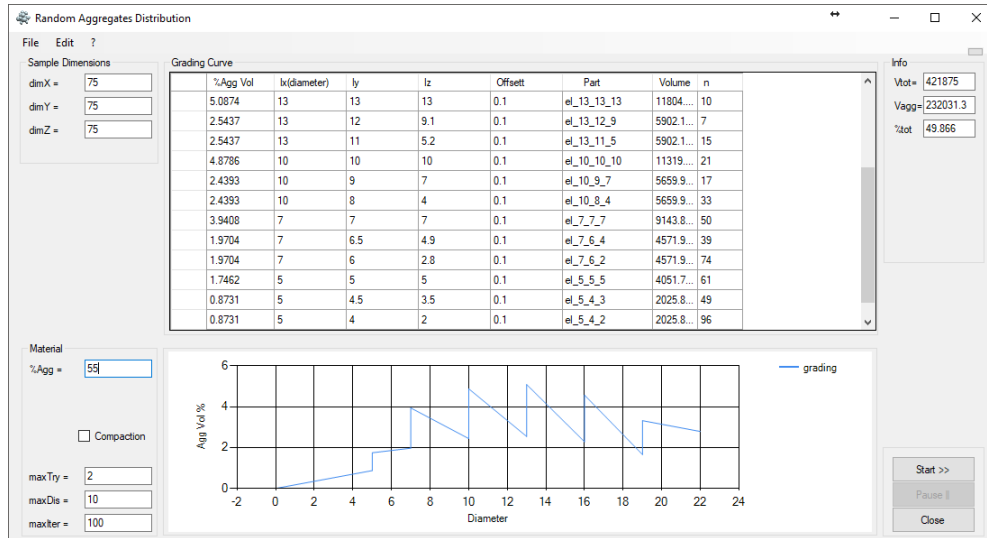
Start >>
Pause ||
Close

Figure 6: Graphical interface of the random generation tool for ellipsoidal inclusions created in *Visual Basic* language.

Once the non-intersecting ellipsoidal mesostructure is characterized in a set of vectors for each inclusion: **o** (centre), **e** (axes orientation) and **l** (axes dimensions), the solid geometry has been generated using the *OPEN CASCADE* library [28], the specific one for CAD processing. Specifically, Phyton programming language has been employed, by means of the *pythonOCC* library [29], which allows to generate ellipsoids of given centre, orientation and dimension (starting from a sphere and scaling it along the three axes) and operate in a Boolean way between solids to dig the sample in correspondence of the inclusions, so to distinguish it from the volume occupied by the aggregates.

An example of the code programmed in Phyton language, generating and visualizing spheres in a sample, is reported in box. 1.

```
for i in range(len(sp)):
    center=gp_Pnt(sp[i][0],sp[i][1],sp[i][2])
    agg = BRepPrimAPI_MakeSphere(center,sp[i][6]/2)
    aggSh = agg.Shape()
    boxTrim = OCC.BRepAlgoAPI.BRepAlgoAPI_Cut(boxSh,aggSh)
    boxSh = boxTrim.Shape()
#-
```

Box 1: sphere generation into the sample in Phyton language using phytonOCC library

The corresponding output is shown in Fig. 7: the sample at the mesoscopic scale is made by coarse aggregates of various dimensions (Fig. 7 a) and the matrix (cement paste and fine aggregate fractions, Fig. 7 b). The matrix has voids in correspondence of the aggregate position in such a way that no solid interference occurs when the two parts are assembled into a unique solid biphasic model and are assigned to them two different material properties.
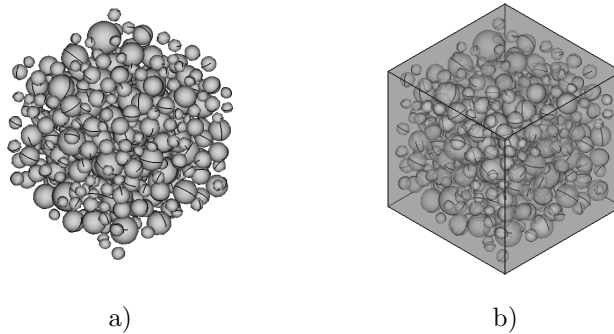

a)   b)

Figure 7: Aggregates a); matrix b).

5. Example

5.1. Concrete with natural gravel aggregates

The efficiency of the algorithm has been tested on the real grading curve reported in [30] for a mix design using natural gravel as aggregates. The coarse

13

fraction has been assumed ranging between 25 mm to 5 mm in diameter, subdivided into the passing fractions reported in Tab. 1. It represents itself the 55% of the total sample volume; from a numerical point of view finer particles are considered embedded into the matrix.

Diameter [mm]	**Passing** [%]
25.0	100.0
16.0	64.3
12.5	46.6
8.0	19.2
4.0	7.9

Table 1: Grading curve of concrete with gravel aggregates, derived from [30].

The grading curve has been divided into 7 different diameters D_i: $\mathbf{D}$=(22 mm; 19 mm; 16 mm; 13 mm; 10 mm; 7 mm; 5 mm) and the corresponding passing percentages have been obtained by interpolatig the data in Tab. 1. A maximum shape ratio $L/E = 2.5$ has been considered and to each nominal D_i three different particles (M_i^0, M_i^1, M_i^2) have been associated, to reasonably differentiate in shape the inclusions: a sphere $(M_i^0$, with $2l_x = 2l_y = 2l_z = D_i)$; an ellipsoid with the maximum allowed shape ratio $(M_i^2$, with $2l_x = D_i; 2l_y = D_{i+1}; 2l_z = D_i/2.5)$ and an ellipsoid M_i^1 with average dimensions between M_i^0 and M_i^2.
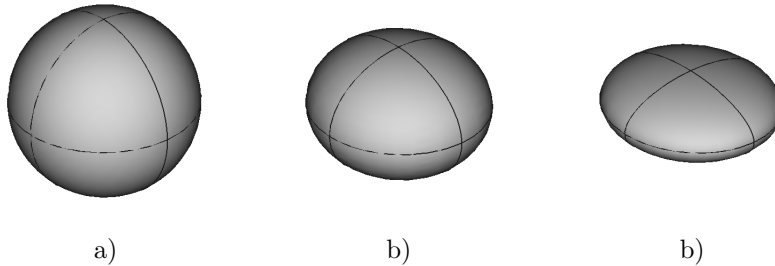

a)   b)   b)

Figure 8: Aggregate-types for a nominal sieve diameter M_i^0 a); M_i^1 b); M_i^2 c).

Each fraction of diameter D_i has a volume V_i determined in relation to the grading curve. The volume fraction for the three ellipsoids $V_{a,i}$ is obtained by defining a frequency parameter for each one of the three ellipsoidal prototypes in the mesostructure, M_i^0, M_i^1, M_i^2, through a coefficient γ, which accounts for the variation in shape of the particles in a same grain fraction. This parameter must be assumed, as in this case, if no information are given on the shape of the aggregates, i.e. in the majority of situations.

Then $V_{a,i} = \gamma V_i$. Particularly, particles M_i^0 have been assumed to fill each volumetric fraction V_i by 50% (i.e. $\gamma = 50\%$), while particles M_i^1 and M_i^2 by 25% of each volume fraction V_i. In principle, any shape at any percentage can be assigned to each V_i.

The parameters characterizing the ellipsoids of each volume fraction are listed in Tab. 2.

D_i	Passing	V_i	γ	$V_{a,i}$	$2l_x$	$2l_y$	$2l_z$	Type
[mm]	[%]	[%]	[%]	[%]	[mm]	[mm]	[mm]	
22	97.21	2.7896	1.00	2.789	22.0	22.0	16.0	M_0^1
19	90.57	6.636	0.50	3.318	19.0	19.0	19.0	M_1^0
			0.25	1.659	19.0	18.0	13.3	M_1^1
			0.25	1.659	19.0	17.0	7.6	M_1^2
16	81.44	9.1344	0.50	4.567	16.0	16.0	16.0	M_2^1
			0.25	2.283	16.0	15.0	11.2	M_2^2
			0.25	2.283	16.0	14.0	6.4	M_2^3
13	71.26	10.1748	0.50	5.087	13.0	13.0	13.0	M_3^1
			0.25	2.543	13.0	12.0	9.1	M_3^2
			0.25	2.543	13.0	11.0	5.2	M_3^3
10	61.50	9.7572	0.50	4.878	10.0	10.0	10.0	M_4^1
			0.25	2.439	10.0	9.0	7.0	M_4^2
			0.25	2.439	10.0	8.0	4.0	M_4^3
7	53.62	7.8816	0.50	3.940	7.0	7.0	7.0	M_5^1
			0.25	1.970	7.0	6.5	4.9	M_5^2
			0.25	1.970	7.0	6.0	2.8	M_5^3
5	50.1	3.4924	0.50	1.746	5.0	5.0	5.0	M_6^1
			0.25	0.873	5.0	4.5	3.5	M_6^2
			0.25	0.873	5.0	4.0	2.0	M_6^3

Table 2: Input data for determinig the expected numerical grading curve of the concrete mix with gravel aggregates characterized in [30].

Only to particles with the biggest diameter ($D_0 = 22$ mm) one unique geometry (M_0^1) has been assigned, due to the low volume fraction, which may be reasonably represented by few particles, if not just one.

225 The data in Tab. 2 are the input data for determining the expected numerical grading curve.

The real grading curve has been reproduced via both ellipsoids of different shape

spheres, to compare the efficiency of the algorithm (Fig. 9). The grading curve has been reconstructed by including the dislocation procedure illustrated above.

230 Since the algorithm necessarily makes use of a maximum number of attempts to insert a new inclusion, $N_{max} = 100$, not all of the expected aggregates can be inserted, so a certain percentage of error is envisaged, compared to the experimental data (real grading curve).
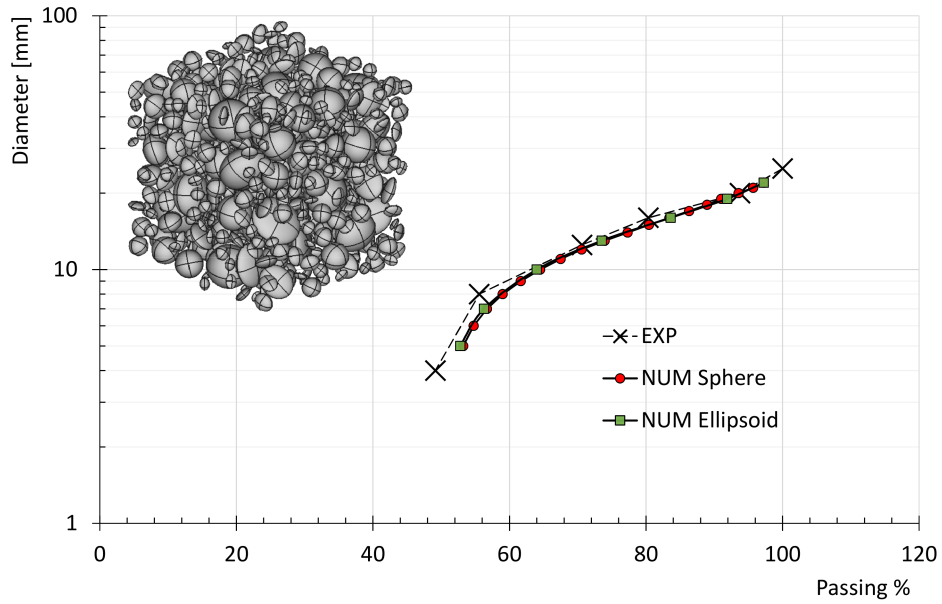

Figure 9: Experimental-numerical comparison of the real and simulated grading curve; experimental results from [30].

The maximum error obtained with ellipsoids occurs in the fine fraction and 235 it is equal to 5%, with an average error of 3%. By using only spheric particles, a more refined distribution of diameters is necessary to estimate the same error, which is computationally more expensive. In this example a diameter variations of 1 mm for spheres has been implemented, in the range $5 - 22$ mm, obviously neglecting in this case the aggregate shape ratio.

240 This result seems also in line with the finding that ellipsoidal inclusions allow to fill a volume in a better way than spheric inclusions.

17

5.2. Concrete with recycled aggregates

Sometimes sustainable solutions are preferred in concrete mix design to preserve natural resources such as gravel. One example is represented by the use of recycled aggregates from demolition waste as an alternative to natural aggregates [20]. They are characterized by a peculiar irregular nature resulting from crushing and a two-phase nature given by the coexistence of originally natural aggregates and attached old mortar. The latter justifies the lower quality of recycled-aggregate concrete obtained by partially or totally replacing natural aggregates with recycled ones.

The use of recycled aggregates has not gained popularity yet but the performance of fresh and hardened recycled-aggregate concrete is being studied extensively, together with new packing methods for this kind of mixes, which are necessary in reason of their lower workability if compared to conventional concrete, as the water absorption capability of the recycled material is higher due to its porous structure [31].

The following example takes into consideration a concrete mix with recycled aggregates satisfying the Bolomey's law, computed for a maximum size of aggregates in the mixture of 22.4 mm and an A coefficient in Equation (2), depending on the shape of the aggregates and on the consistency of the class, equal to 12 [32].

The mixture is composed by 350 kg/m^3 of cement CEM I 52.5R with a w/c ratio equal to 0.45. The global volume of aggregates is distributed as follows: 9.2% of recycled aggregates, 39.8% of coarse natural aggregates (gravel) and 51% of fine natural aggregates (sand), the overall aggregates representing 73% of the total sample volume, with the coarse fraction equal to 36% of the total aggregate volume.

The grading curve of the coarse fraction is reported in Tab. 3.

18

Diameter [mm]	Passing [%]
16.0	100.0
14.0	93.3
12.5	88.0
10.0	78.3
8.0	69.6
6.3	61.4

Table 3: Grading curve of a concrete with recycled aggregates.

The algorithm, inclusive of the dislocation procedure, has been used to reproduce the real grading curve with spheric particles only. This example compares the results obtained by considering two possible maximum numbers of attempts to collocate an inclusion, i.e. 100 and 150.

The comparison between the real and the numerical solution (Fig. 10) shows again a fairly good agreement, despite the expected irregular shape of these type of aggregates partially included in the mix.

The grading curve has been divided into 11 different aggregate diameters, with dimension ranging from 15 to 5 mm, with an interval of 1 mm; the maximum volume fraction at each diameter has been obtained by interpolating the passing through each sieve reported in Tab. 3.
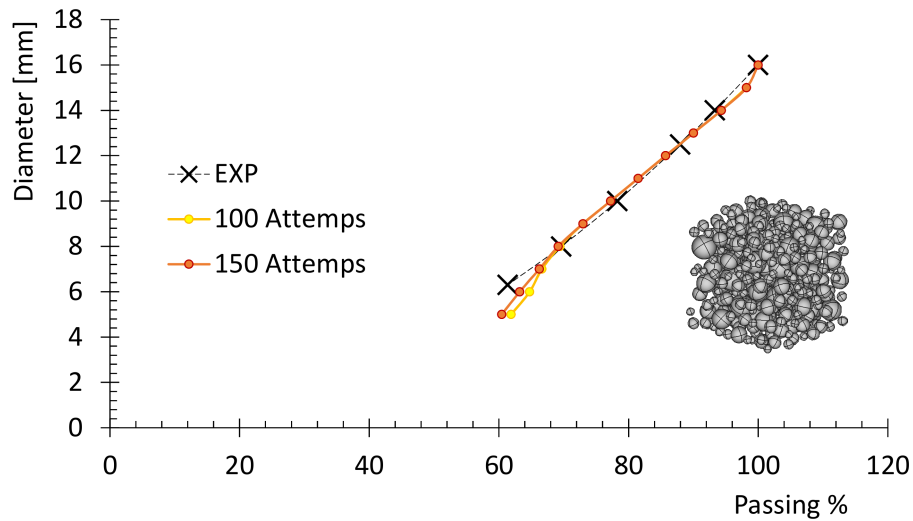
Figure 10: Experimental-numerical comparison of the real and simulated grading curve of a concrete mix with recycled aggregates.

The maximum error is again encountered in placing the finest aggregates, equal to 6.7% for the optimal algorithm considering 150 maximum attempts, with an average error equal to only 1.62%. Despite the negligible increase in the number of attempts, the higher N_{max} the more reliable the simulated grain packing.

Conclusions

An algorithm to randomly distribute in space ellipsoidal inclusions and in agreement with real grading curves for concrete materials has been outlined; the simulated packing densities are proved to be very close to the experimental values both for regular round aggregates, which can be better approximated with ellipsoids, and aggregates of irregular shape, like crushed particles from demolition waste.
The novelty of the approach stands on the dislocation procedure introduced into the algorithm to minimize voids and enhance packing between particles without overlapping.

20

The same algorithm applied to polydispersed spheres reaches similar packing density values, though with a more refined grain size distribution in input if compared to ellipsoidal inclusions, which is more expensive from the computational point of view.

Such an algorithm appears to be particularly suitable for being implemented into FE codes devoted to analyse composite materials via continuum models.

References

[1] H. He, Z. Guo, P. Stroeven, M. Stroeven, L.J. Sluys, Characterization of the packing of aggregate in concrete by a discrete element approach, Mater. Charact. 60 (2009) 1082-1087.

[2] W.X. Xu, H. Chen, Microstructural modelling of cement-based materials via random packing of three-dimensional ellipsoidal particles, Procedia Engineer. 27 (2012) 332-340.

[3] W.X. Xu, H.S. Chen, Z. Lv, An overlapping detection algorithm for random sequential packing of elliptical particles, Physica A 390 (2011) 2452-2467.

[4] C.C. Furnas, Grading aggregates I−mathematical relations for beds of broken solids of maximum density, Ind. Eng. Chem. 23 (9) (1931) 1052-1058.

[5] T. Stovall, F. de Larrard, M. Buil, Linear packing density model of grain mixtures, Powder Technol. 48 (1986) 1-12.

[6] D.P. Bentz, E.J. Garboczi, Percolation of phase in a three-dimensional cement paste microstructural model, Cem. Concr. Res. 21 (1991) 325-344.

[7] K. Sobolev, A. Amirjanov, Application of genetic algorithm for modeling of dense packing of concrete aggregates, Constr. Build. Mater. 24 (2010) 1449-1455.

[8] M.V. Pathan, V.L. Tagarielli, S. Patsias, P.M. Baiz-Villafranca, A new algorithm to generate representative volume elements of composites with cylindrical or spherical fillers, Compos. Part B-Eng. 110 (2017) 267-278.

[9] F.H. Wittmann, P.E. Roelfstra, H. Sadouki, Simulation and analysis of composite structures, Mater. Sci. Engng. 68 (1984) 239-648.

[10] J.K. Beddow, T. Meloy, Testing and characterization of powders and fine particles. London, Heyden, 1980.

[11] Z.M. Wang, A.K.H. Kwan, H.C. Chan, Mesoscopic study of concrete I: generation of random aggregate structure and finite element mesh, Comput. Struct. 70 (1999) 533-544.

[12] E.J. Garboczi, K.A. Snyder, J.F. Douglas, M.F. Thorpe, Geometrical percolation threshold of overlapping ellipsoids, Phys. Rev. E. 52 (1995) 819-828.

[13] J.D. Sherwood, Packing of spheroids in three-dimensional space by random sequential addition, J. Phys. A: Math. Gen. 30 (1997) 839-943.

[14] X. Lin, T.T. Ng, A three-dimensional discrete element model using arrays of ellipsoids. Geotechnique, 47 (2) (1997) 319-329.

[15] S. Hafner, S. Eckardt, T. Luther, C. Konke, Mesoscale modeling of concrete: geometry and numerics, Comput. Struct. 84 (2006) 450-461.

[16] S.R. Williams, A.P. Philipse, Random packings of spheres and spherocylinders simulated by mechanical contraction, Phys. Rev. E 67 (2003) 1-9.

[17] Z.P. Bazant, M.R. Tabbara, M.T. Kazemi, G. Pijaudier-Cabot, Random particle model for fracture of aggregate or fiber composites, J. Engng. Mech. 116 (8) (1990) 1686-1705.

[18] G. De Schutter, L. Taerwe, Random particle model for concrete based on Delaunay triangulation, Mater. Struct. 26 (1993) 67-73.

[19] T.P. Runarsson, X. Yao, Stochastic ranking for constrained evolutionary optimization, IEEE Trans. Evolut. Comput. 4 (3) (2000) 284-294.

22

[20] G. Mazzucco, G. Xotta, B. Pomaro, V.A. Salomoni, F. Faleschini, Elastoplastic-damaged meso-scale modeling of concrete with recycled aggregates, in press in Compos. Part B-Eng. (2017).

[21] W.B. Fuller, S.E. Thompson, The laws of proportioning concrete, ASCE J. Transactions 59 (2) (1907) 67-143.

[22] J. Bolomey, Granulation et prévision de la résistance probable des bétons, Travaux 19 (30) (1935) 228-232.

[23] UNI EN 933-4 - Tests for geometrical properties of aggregates − Determination of particle shape − Shape index, 2008.

[24] T. Larsson, An efficient ellipsoid-OBB intersection test. Journal of Graphics, GPU, and Game Tools 13 (1) (2008) 31-43.

[25] S. Alfano, M.L. Greer, Determining if two solid ellipsoids intersect, J. Guid. Control Dynam. 26 (1) (2003) 106-110.

[26] W. Wang, J. Wang, M.S. Kim, An algebraic condition for the separation of two ellipsoids, Comput. Aided Geom. D 18 (2001) 531-539.

[27] S. Torquato, Random heterogeneous materials: microstructure and macroscopic properties. Springer-Verlag, New York, 2002.

[28] https://www.opencascade.com/

[29] http://www.pythonocc.org/

[30] M. Cetraro, S. De Paola, M. Massaccesi, G. Menditto, G. Porco, Curve di correlazione per il controllo della affidabilit dei calcestruzzi ordinari [Correlation curves for reliability assessment of ordinary concretes]. In: Calcestruzzi autocompattanti: progettazione, produzione e controlli sperimentali, Centro Studi e Ricerche Sposato P&P srl, Sibari (CS) Italy, 9, 2003.

[31] S. Pradhan, S. Kumar, S.V. Barai, Recycled aggregate concrete: Particle Packing Method (PPM) of mix design approach, Constr Build Mater. 152 (2017) 269-284.

[32] G. Mazzucco, G. Xotta, B. Pomaro, C.E. Majorana, F. Faleschini, C. Pellegrino, Mesoscale Modelling of Concrete with Recycled Aggregates. In: 10th International Conference on Mechanics and Physics of Creep, Shrinkage, and Durability of Concrete and Concrete Structures, September 2015.